AMERICAN SOCIETY FOR MICROBIOLOGY | Applied and Environmental Microbiology®

BIOTECHNOLOGY

Discovery of Polyesterases from Moss-Associated Microorganisms

Christina Andrea Müller,[a,b] Veronika Perz,[c] Christoph Provasnek,[a,b] Felice Quartinello,[d] Georg M. Guebitz,[c,d] Gabriele Berg[a]

Institute of Environmental Biotechnology, Graz University of Technology, Graz, Austria[a]; ACIB GmbH, Graz, Austria[b]; ACIB GmbH, Tulln an der Donau, Austria[c]; Institute of Environmental Biotechnology, University of Natural Resources and Life Sciences, Tulln an der Donau, Austria[d]

ABSTRACT The growing pollution of the environment with plastic debris is a global threat which urgently requires biotechnological solutions. Enzymatic recycling not only prevents pollution but also would allow recovery of valuable building blocks. Therefore, we explored the existence of microbial polyesterases in microbial communities associated with the *Sphagnum magellanicum* moss, a key species within unexploited bog ecosystems. This resulted in the identification of six novel esterases, which were isolated, cloned, and heterologously expressed in *Escherichia coli*. The esterases were found to hydrolyze the copolyester poly(butylene adipate-*co*-butylene terephthalate) (PBAT) and the oligomeric model substrate bis[4-(benzoyloxy)butyl] terephthalate (BaBTaBBa). Two promising polyesterase candidates, EstB3 and EstC7, which clustered in family VIII of bacterial lipolytic enzymes, were purified and characterized using the soluble esterase substrate *p*-nitrophenyl butyrate (K_m values of 46.5 and 3.4 μM, temperature optima of 48°C and 50°C, and pH optima of 7.0 and 8.5, respectively). In particular, EstC7 showed outstanding activity and a strong preference for hydrolysis of the aromatic ester bond in PBAT. Our study highlights the potential of plant-associated microbiomes from extreme natural ecosystems as a source for novel hydrolytic enzymes hydrolyzing polymeric compounds.

IMPORTANCE In this study, we describe the discovery and analysis of new enzymes from microbial communities associated with plants (moss). The recovered enzymes show the ability to hydrolyze not only common esterase substrates but also the synthetic polyester poly(butylene adipate-*co*-butylene terephthalate), which is a common material employed in biodegradable plastics. The widespread use of such synthetic polyesters in industry and society requires the development of new sustainable technological solutions for their recycling. The discovered enzymes have the potential to be used as catalysts for selective recovery of valuable building blocks from this material.

KEYWORDS enzyme discovery, esterases, functional metagenomics, plant-associated microbiomes, polymer hydrolysis

Received 22 September 2016 **Accepted** 7 December 2016

Accepted manuscript posted online 9 December 2016

Citation Müller CA, Perz V, Provasnek C, Quartinello F, Guebitz GM, Berg G. 2017. Discovery of polyesterases from moss-associated microorganisms. Appl Environ Microbiol 83:e02641-16. https://doi.org/10.1128/AEM.02641-16.

Editor Haruyuki Atomi, Kyoto University

Copyright © 2017 American Society for Microbiology. All Rights Reserved.

Address correspondence to Christina Andrea Müller, christina.mueller@tugraz.at.

C.A.M. and V.P. are co-first authors.

Different types of natural aliphatic polyesters can be found in nature, such as poly-3-hydroxybutyrate and other polyhydroxyalkanoates produced by bacteria (1) and cutin, a main component of the cuticle in higher plants (2). In addition to these natural polyesters, several types of synthetic polyesters, mainly aliphatic polyesters and aliphatic-aromatic copolyesters, have been developed in the past century (3). Some synthetic polyesters have characteristics and chemical structures that allow good biodegradability; however, the most popular and widespread polyesters, namely, polyethylene terephthalate (PET) and polybutylene terephthalate (PBT), exhibit rather restricted biodegradability and were long considered to be resistant to microbial attack

Downloaded from http://aem.asm.org/ on May 5, 2018 by guest

(4). The increasing pollution of nature with microplastic debris is a global threat and a key challenge for future generations (5, 6). Biodegradation of polyesters is a heterogeneous process consisting of initial depolymerization to water-soluble intermediates by extracellular enzymes and subsequent assimilation of intermediates into metabolic pathways to achieve final degradation (4). The initial depolymerization is considered the limiting biodegradation step (4). Systematic studies by Marten et al. revealed that the mobility of the polymer chains is the key factor affecting the biodegradability of aliphatic and aromatic polyesters (7, 8). By combining aliphatic and aromatic monomers in the synthesis of copolyesters, it is possible to achieve greater biodegradability while keeping the material properties acceptable (8). The copolyester poly(butylene adipate-*co*-butylene terephthalate) (PBAT), for instance, belongs to this category. PBAT is synthetized on an industrial scale by several companies, through polycondensation of the aliphatic monomers adipic acid (Ada) and 1,4-butanediol (B) and the aromatic monomer terephthalic acid (Ta) (9). PBAT can also be used as a component of polymer blends with, for example, poly(lactic acid) (PLA) (10).

The ever-growing use of plastic-based materials strengthens the need to investigate not only biodegradable polyesters but also microorganisms and whole microbiomes for new enzymes. Novel biocatalysts capable of hydrolyzing polyesters could allow recycling of valuable building blocks. Microbial enzymes from various sources (e.g., compost) that can degrade or modify natural and synthetic polyesters have been studied previously (11, 12). Esterases and lipases not only are prevalent in most natural ecosystems and microorganisms but also are some of the most widely used biocatalysts in the chemical industry (13). According to the family classification system defined first by Arpigny and Jaeger (14), bacterial esterases and lipases can be grouped into lipolytic enzyme families I to VIII. This classification system was later extended up to family XIV (15). Several hydrolases with polyester-degrading capabilities have been isolated from bacteria belonging to the phyla *Actinobacteria* (e.g., *Thermobifida* spp. and *Saccharomonospora viridis*), *Proteobacteria* (*Pseudomonas mendocina*), and *Firmicutes* (e.g., *Bacillus subtilis* and *Clostridium* spp.) and from fungi (e.g., *Fusarium solani*, *Humicola insolens*, *Aspergillus oryzae*, and *Rhizopus* spp.) (6, 11, 16–21). While searching for new microorganisms, Yoshida et al. recently discovered the novel bacterium *Ideonella sakaiensis*, which contains two PET hydrolases and is capable of utilizing PET as an energy and carbon source (22). It was demonstrated that metagenomes are also promising sources for novel enzymes (23). However, there are only seven examples of polyester-hydrolyzing enzymes from metagenomic sources, including the LC-cutinase from a leaf-branch compost metagenomic library, which is capable of hydrolyzing not only cutin but also PET (24), the PLA depolymerase PlaM4, which is also from a compost metagenome (25), and five esterases from marine metagenomic libraries with hydrolytic activities toward several polyester substrates, including PLA (26). The potential of plant-associated metagenomes as a source of novel enzymatic activities has been less well explored (27).

The objective of our study was to explore the *Sphagnum* bog metagenome for identification of novel enzymatic activities. *Sphagnum magellanicum* is the dominant species in bog ecosystems. It has been shown that the *Sphagnum* microbiome supports the host in terms of metabolism, growth, and health (28), as well as ecosystem functioning under extreme conditions (29–31). In contrast to the reported low enzymatic activities in the anaerobic areas of bogs (32, 33), analysis of the *Sphagnum* moss metagenome revealed very high levels of taxonomic and functional diversity (31). The influence of specialized microorganisms, harboring novel enzymes, on ecosystem functioning was also reported for peatland soils (34). The cell wall components of *Sphagnum* leaves contain polysaccharides similar to those found in higher plants, possibly cellulose, mannans, xylans (35), pectin-like polysaccharides, xyloglucans, and uronic acid (36). Moreover, extracts of different moss species, including *Sphagnum magellanicum*, also contain high concentrations of secondary metabolites such as sterols, polyphenols, and terpenoids (37). Based on the tight interactions and functional diversity of the *Sphagnum* moss microbiome, we expected significant abundance and

Downloaded from http://aem.asm.org/ on May 5, 2018 by guest

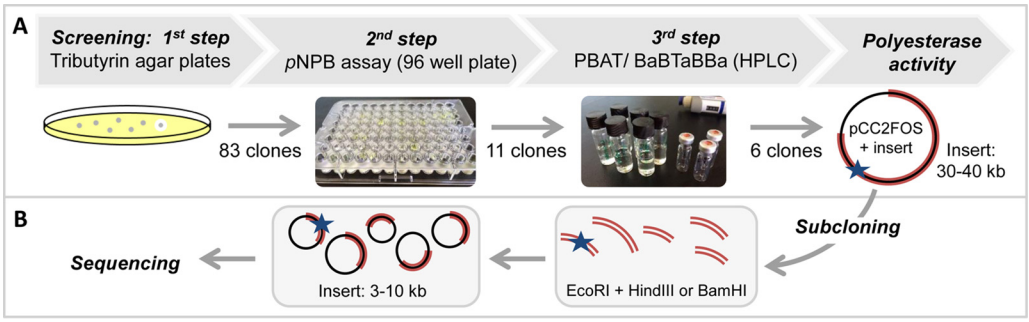


FIG 1 Schematic presentation of the screening process for metagenome-derived clones showing polyester-hydrolyzing activity and retrieval of sequences. (A) Three screening steps for identification of fosmid clones containing the target hydrolytic activity, as follows: first step, tributyrin agar plates; second step, pNPB assay in 96-well plates; third step, HPLC analysis of PBAT and BaBTaBBa reaction products. Positively identified clones harbor the library vector pCC2FOS containing the metagenome insert DNA with the targeted hydrolase gene (marked with a star). (B) Subcloning of shorter insert DNA fragments after digestion with restriction enzymes (EcoRI and HindIII or BamHI). Subclones displaying the same hydrolytic activity were sequenced for identification of the hydrolase ORF.

high levels of diversity of hydrolases that play essential roles in plant metabolism, especially in regard to degradation and/or assimilation of plant polysaccharides, polymers, and secondary metabolites, while exhibiting hydrolytic activities toward synthetic polymers.

RESULTS AND DISCUSSION

Screening for esterases in the *Sphagnum* moss metagenome. In order to identify enzymes for hydrolysis of aromatic-aliphatic polyesters, we investigated the microbiome associated with the moss *Sphagnum magellanicum* as a source for esterases. Our screening strategy consisted of three steps (Fig. 1), allowing identification of clones displaying not only esterase activity but also, in particular, polyester-hydrolyzing activity.

The initial high-throughput screening of around 90,000 fosmid clones from the moss metagenome library resulted in identification of 83 clones showing hydrolytic activity (halo formation) on tributyrin agar plates (Fig. 1A and data not shown). During the second screening step, the 83 identified clones were evaluated for hydrolytic activity toward *p*-nitrophenyl butyrate (*p*NPB) by using cell-free lysates (see Table S2 in the supplemental material). The 11 most active clones were selected for a third screening step using two different synthetic copolyesters. In addition, cell-free lysates were tested for the presence of hydrolases by labeling active serine hydrolases in the samples with a fluorogenic probe prior to SDS-PAGE analysis (Fig. S1); this allowed detection of distinct and significantly intense hydrolase bands in the analyzed clones with molecular masses of 30 to 50 kDa, providing evidence for the presence of putative esterases. Finally, six nonredundant clones (clones B3, B11, C5, C7, C9, and G4) showed significant hydrolytic activity with the aliphatic-aromatic copolyester PBAT (ecoflex; BASF) and the oligomeric low-molecular-weight PBAT model substrate bis[4-(benzoyloxy)butyl] terephthalate (BaBTaBBa), compared to the control reaction (library host carrying the empty vector) (Fig. S2).

Identification and classification of metagenome esterases. Subcloning of the 6 fosmid clones with polyester-hydrolyzing activities was performed to gain shorter DNA fragments for sequencing (Fig. 1B). The sequencing results allowed identification of open reading frames (ORFs) coding for putative esterases. The esterases coded by the six individual ORFs were termed EstB3, EstB11, EstC5, EstC7, EstC9, and EstG4. Table 1 shows characteristic properties of the six esterase coding sequences.

Gene lengths ranged between 888 and 1,227 bp, showing rather high GC contents of 62.2 to 65.1%, with the exception of EstG4 (40.3%). Possible N-terminal signal peptides were predicted for the ORFs of EstC5 and EstG4 using SignalP 4.1 software (38). Sequence similarities among the six esterases were estimated by alignment and

Downloaded from http://aem.asm.org/ on May 5, 2018 by guest

TABLE 1 Properties of identified ORFs and protein coding sequences (wild type) for six novel metagenome esterases

ORF	Length (bp)	GC content (%)	Protein sequence				
			Size (amino acids)	Estimated molecular mass (kDa)	Predicted isoelectric point	Predicted signal peptide[a]	Maximal amino acid sequence identity (GenBank accession no.)[b]
EstB3	1,227	64.9	408	44.54	6.28	No	63% vs serine hydrolase from *Tardiphaga* sp. Vaf07 (WP_068735481)
EstB11	1,152	62.2	383	40.31	5.33	No	55% vs 1,4-butanediol diacrylate esterase from *Thermorudis peleae* (WP_038038941)
EstC5	918	63.9	305	32.76	6.50	N-terminal (~34 amino acids)	61% vs esterase/lipase from *Caulobacter vibrioides* (WP_004617716)
EstC7	1,155	63.6	383	40.20	5.43	No	53% vs 1,4-butanediol diacrylate esterase from *Thermorudis peleae* (WP_038038941)
EstC9	888	65.1	295	30.82	7.78	No	56% vs α/β-hydrolase from *Acidocella* sp. MX-AZ02 (WP_008494015)
EstG4	960	40.3	319	35.80	5.61	N-terminal (~19 amino acids)	37% vs hypothetical protein ACD_45C00716G0002 from uncultured bacterium (EKD72285)

[a]Signal peptide prediction was performed with SignalP 4.1, with a cutoff value for discrimination scores of 0.500.
[b]BLASTP analysis against the GenBank database of full-length nonredundant protein sequences (23 August 2016 version) yielded the maximal identity to the closest annotated hit.

pairwise comparison of amino acid sequences. EstB11 and EstC7 had the greatest sequence identity (69.8%), followed by lower levels of identity between EstB3 and EstC7 (29.9%), EstB3 and EstB11 (27.5%), and EstC5 and EstC9 (24.7%). All other sequence pairs demonstrated levels of identity below 14.4%.

Phylogenetic analysis of the ORF sequences revealed amino acid sequence homology with annotated esterases from the GenBank protein database of 37 to 63% (Table 1). Multiple sequence alignments of the six metagenome esterases and reference sequences belonging to all 14 known lipolytic families revealed the presence of conserved esterase motifs (Fig. S3). Based on phylogenetic analysis, the metagenome esterases could be classified into three previously reported families (see the phylogenetic tree in Fig. S4).

EstB3, EstB11, and EstC7 clustered into family VIII of carboxylesterases, which share sequence identity with class C β-lactamases and penicillin-binding proteins (14). They harbor an active site serine residue in the consensus sequence SMTK (SXXK motif), with a catalytic triad of Ser-Lys-Tyr, comparable to the other enzymes in this family and especially the recently reported crystal structure of EstU1 (PDB accession no. 4IVK) (39). Promiscuous β-lactamase activity has been demonstrated for some members of this family, such as the metagenome-derived carboxylesterases EstU1 (40) and Est22 (41), with first-generation cephalosporin-based derivatives. EstG4 clustered in family II of lipolytic enzymes, which show the conserved motif GDSL containing the active site serine. In this family, the catalytic triad is the classic Ser-Asp-His sequence found in α/β-hydrolases (42). EstC5 and EstC9 showed similarities to enzymes grouped into family IV, which contains hormone-sensitive lipase (HSL)-like esterases that display the conserved pentapeptide motif GXSXG, containing the active site serine (43). EstC5 shows the typical triad Ser-Asp-His, while EstC9 may utilize glutamic acid (Ser-Glu-His) instead of aspartic acid. To compare the affiliations of the metagenome esterases with those of previously characterized polyesterases with documented activity toward PBAT, the following enzymes were included in the phylogenetic analysis: esterases Cbotu_EstA, Cbotu_EstB (*Clostridium botulinum*) (20), and Chath_Est1 (*Clostridium hathewayi*) (21), lipase Pfl1 (*Pelosinus fermentans*) (44), and cutinases Cut190 (*Saccharomonosporas viridis*) (19) and Thc_Cut1 (*Thermobifida cellulosilytica*) (45). These six known PBAT hydrolases share the same catalytic triad Ser-Asp-His (or Ser-Glu-His, in the case of Chath_Est1). Cbotu_EstA, Cbotu_EstB (conserved motif GHSMGG), and Pfl1 (AHSMG) do not directly cluster with any of the 14 reported lipolytic enzyme families and seem to represent a new cluster of lipolytic enzymes in close proximity to families I, V, and IX. In contrast, the esterase Chath_Est1 (GQSGG) clusters in family VII and the

Downloaded from http://aem.asm.org/ on May 5, 2018 by guest

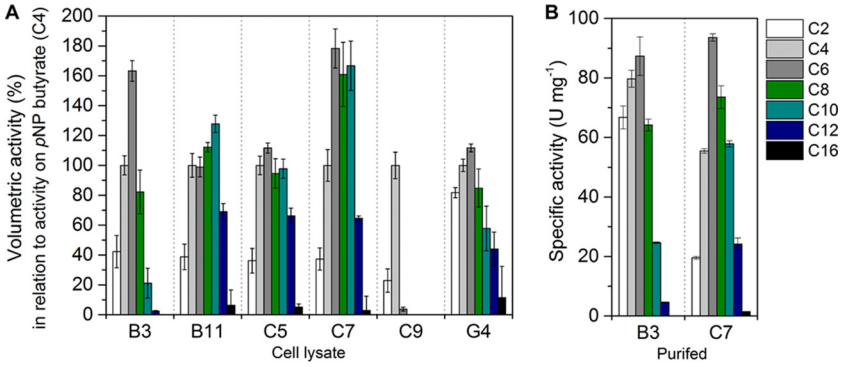


FIG 2 Substrate profiles of metagenome esterases, as either cell-free lysates (A) or purified enzymes (B), using *p*NP aliphatic esters with various chain lengths. The *p*NP aliphatic esters were *p*NP acetate (C_2), *p*NPB (C_4), *p*NP hexanoate (C_6), *p*NP octanoate (C_8), *p*NP decanoate (C_{10}), *p*NP dodecanoate (C_{12}), and *p*NP palmitate (C_{16}). Bars, mean values of at least 2 measurements; error bars, standard deviations.

cutinases Cut190 and Thc_Cut1 (GXSMG) in family III. The phylogenetic analysis indicated that the previously reported PBAT-degrading enzymes are not affiliated with the same lipolytic families as the esterases discovered in this study. Therefore, the observed polyesterase activities do not seem to be strictly dependent on sequence similarity.

Substrate profiles and thermostability of cloned esterases. The six metagenome esterase genes were cloned into *E. coli* BL21(DE3) or Lemo21(DE3) using the inducible vector pET28a(+). Heterologous expression of soluble enzymes was confirmed by SDS-PAGE analysis and visualization using a fluorogenic serine hydrolase label (Fig. S5). Substrate specificity profiles of the cloned esterases were measured using cell-free lysates and *p*-nitrophenyl (*p*NP) aliphatic esters of different chain lengths (Fig. 2A). To enable comparison of the substrate profiles despite strong differences in the expression levels of the esterases in the cell-free lysates, volumetric activities were calculated as percentages of the activity measured with the commonly employed reference substrate *p*NPB. In the cases of EstB3 and EstC7, substrate profiles were also recorded with purified enzyme (Fig. 2B).

All six esterases showed strong preferences for substrates with short (C_2 to C_4) or medium (C_6 to C_{10}) chain lengths. The smallest substrate (*p*NP acetate [C_2]) was accepted by all esterases, while the largest tested substrate (*p*NP palmitate [C_{16}]) was converted only by EstB11, EstC5, EstC7, and EstG4. The esterases EstB3, EstC5, EstC7, and EstG4 showed their highest hydrolysis rates with *p*NP hexanoate (C_6), while EstB11 was more active with *p*NP decanoate (C_{10}) and EstC9 preferentially hydrolyzed *p*NPB (C_4). The substrate profiles were corroborated for EstB3 and EStC7 using purified enzymes. Based on the substrate profiles, it can be concluded that the identified enzymes displayed esterase character, belonging to the group of true esterases. The six moss metagenome esterases presented here showed clear differences in their substrate profiles. The majority of metagenome-derived esterases discovered to date also show preferences for short-chain to medium-chain *p*-nitrophenyl aliphatic esters (46).

The thermostability of the esterases in the cell-free lysates was evaluated for a period of at least 96 h. The stability was measured as residual activity at 30°C and 50°C using the *p*NPB assay (Fig. S6). During incubation for 96 h at 30°C, no significant loss of hydrolytic activity was observed for the six esterases. At 50°C, the esterases in lysates B3, B11, C5, C7, and C9 were quickly inactivated. In contrast to the other esterases, esterase G4 showed a high level of stability at 50°C during a prolonged incubation of 96 h, without a decrease in residual activity. Control samples (cell-free lysates of *E. coli* carrying the empty vector) did not show any significant activity. Due to the excellent stability of all six esterases at 30°C for 72 h, the hydrolysis experiments with PBAT were performed at this temperature.

Activity with the polyester PBAT. In addition to the activities determined with the common soluble ester substrates, the hydrolysis of the polyester PBAT and the more

Downloaded from http://aem.asm.org/ on May 5, 2018 by guest

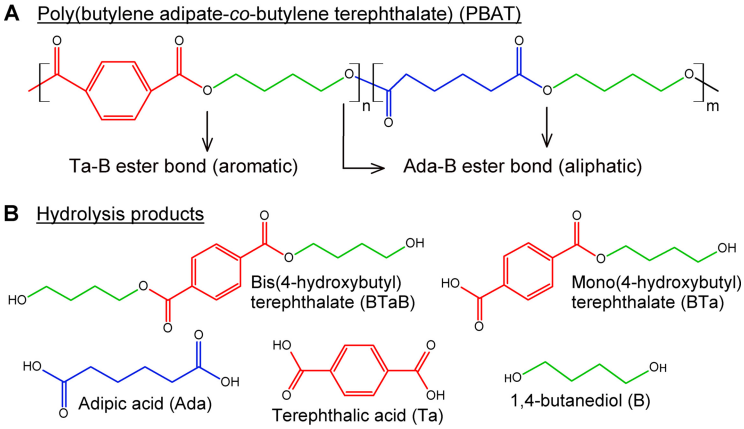


FIG 3 Chemical structure (A) and enzymatic hydrolysis (B) of the aliphatic-aromatic copolyester PBAT. PBAT contains an adipic acid/terephthalic acid ratio of approximately 50:50. Possible hydrolysis products are BTaB, BTa, B, Ada, and Ta.

persistent polyester PET was investigated. Our goal was to evaluate the potential of each metagenome esterase for polyester degradation and to select the best degraders for further study. The polyester cleavage pattern depends on each enzyme's specificity and its ability to accommodate the less-flexible, high-molecular-weight aliphatic-aromatic copolyester chain in the enzyme's active site (8). Enzymatic hydrolysis of PBAT (Fig. 3) leads to the release of the possible hydrolytic products Ada, bis(4-hydroxybutyl) terephthalate (BTaB), and B, resulting from hydrolysis of the aliphatic ester bonds, as well as mono(4-hydroxybutyl) terephthalate (BTa) and Ta, resulting from hydrolysis of the aromatic ester bonds.

The polyester was applied to the reactions in two different forms, i.e., either as milled powder (Fig. 4A) or as a piece of polyester foil (Fig. 4B). Product quantification by means of reverse-phase high-performance liquid chromatography (RP-HPLC) with UV-visible (UV-Vis) detection focused on detection of the most important products from hydrolytic cleavage of the aromatic ester bond, namely, Ta and the Ta-containing oligomers BTa and BTaB.

Generally, higher concentrations of Ta versus BTaB and BTa indicate more efficient enzymatic hydrolysis of the aromatic ester bond, i.e., the Ta-B bond (12). The highest concentrations of released Ta (up to 35 μM) were measured with milled PBAT and EstB3, EstB11, and EstC7 (Fig. 4A). In contrast, EstC5 and EstC9 showed minor accumulation of BTa and BTaB with both substrate forms but poor or no release of Ta. Moreover, the hydrolytic activity of EstG4 toward PBAT was negligible in both cases. To

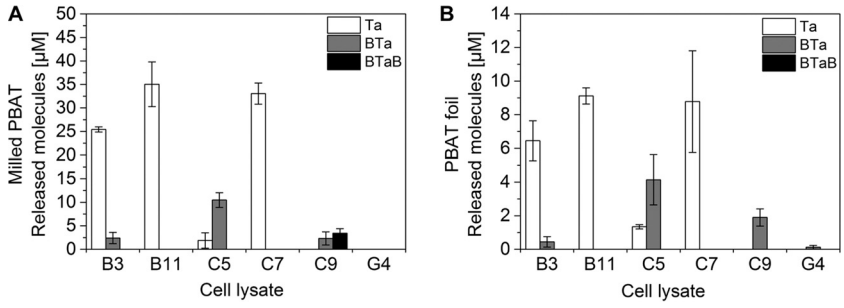


FIG 4 Hydrolysis of PBAT by cell-free lysates from strains containing heterologous expressed esterases from the *Sphagnum* moss metagenome. Reactions with milled PBAT (A) and PBAT foil (B) were performed as described in Materials and Methods (2-ml reaction mixtures at pH 7.5, with incubation at 30°C and 100 rpm for 72 h). The hydrolytic products Ta, BTa, and BTaB were quantified by HPLC/UV-Vis analysis. Values for hydrolysis products released during control and blank reactions were subtracted in order to exclude the influence of hydrolytic enzymes from the *E. coli* host. Bars, mean values (n = 3); error bars, standard deviations.

Downloaded from http://aem.asm.org/ on May 5, 2018 by guest

exclude the influence of hydrolytic activities of other enzymes present in the cell-free lysates, values for control and blank reactions were subtracted from those for the measured samples; however, it was not possible to exclude synergistic effects of the heterologous expressed esterases and the native enzymatic activity of *E. coli* during hydrolysis of the polyester.

Esterases displaying higher concentrations of released Ta are of special interest, since the enzymatic cleavage of aromatic ester bonds in a polyester chain is more difficult to achieve than the cleavage of aliphatic ester bonds, due to lower chain mobility and melting temperatures (3, 7, 8). Released Ta concentrations were nearly 4-fold higher after incubation of the same enzymes with PBAT applied as milled particles, in contrast to PBAT foil (Fig. 4B). The higher activity levels with milled and resuspended PBAT particles is not surprising, since the particles offer greater surface area for enzyme attachment and consequently greater amounts of exposed substrate chains for catalytic attack than does the PBAT foil. Unfortunately, no significant amounts of hydrolysis products could be measured for the reaction mixtures containing PET foil. Interestingly, the three esterases (EstB3, EstB11, and EstC7) that exhibited high levels of activity with PBAT belong to the same family of lipolytic enzymes, i.e., family VIII, which has a different catalytic triad (Ser-Lys-Tyr), compared to the classic Ser-Asp/Glu-His triad found in the previously characterized PBAT hydrolases Thc_Cut1, Cbotu_A, Cbotu_B, Pfl1, Cut190, and Chath_Est1 (19–21, 44, 45). In summary, the esterases EstB3, EstB11, and EstC7 showed higher levels of activity in polyester hydrolysis than did EstC5, EstC9, and EstG4 and therefore are the most promising candidates for further study.

Kinetic characterization of purified EstB3 and EstC7. The esterases EstB3, EstB11, and EstC7 showed significant hydrolytic activity with PBAT during prescreening experiments. For that reason, these enzymes were selected for purification by affinity chromatography with Ni-Sepharose columns, using the N-terminal His-tagged proteins. Purification of EstB3 and EstC7 was achieved with purities of >98%, as estimated by SDS-PAGE analysis (Fig. S7). Unfortunately, His tag purification of EstB11 was not successful under several conditions. Therefore, this study focused on characterization of purified EstB3 and EstC7, in terms of kinetic parameters and hydrolysis of the PBAT polyester.

The kinetic data for EstC7 were fitted according to the Michaelis-Menten equation, resulting in a V_{max} of 70.6 U mg^{-1} and a K_m of 3.43 μM. The best fitting of the EstB3 kinetic parameters was achieved by using the Hill equation instead of the Michaelis-Menten equation, and n_H was estimated to be 0.687. V_{max} and K_m values for EstB3 were 340.8 U mg^{-1} and 46.45 μM, respectively. The K_m values determined for EstB3 and EstC7 were very low, suggesting high affinity for *p*NPB as a substrate. For comparison, K_m values for other family VIII carboxylesterases from metagenome sources, such as those for EstC (58.7 μM) (47) and EstU1 (6.0 μM) (40), are in a similar range. The recently described esterase Cbotu_EstA, which is also capable of hydrolyzing PBAT, has a V_{max} value similar to that of EstC7 (Cbotu_EstA V_{max} = 83.4 U mg^{-1}); however, the K_m value for Cbotu_EstA is 3 orders of magnitude higher (1.95 mM) (20). Lower K_m values for *p*NPB were reported for the eukaryotic liver carboxylesterases from sheep (*Ovis aries*) (0.43 μM), chicken (*Gallus gallus*) (0.55 μM), and horse (*Equus caballus*) (1.1 μM) (48).

The temperature and pH profiles of EstB3 and EstC7 were determined as well (Fig. 5). For the temperature profiles, the standard *p*NPB assay was used. Determination of pH profiles with the chromogenic substrate *p*NPB was not feasible at pH values higher than 9.0, due to rapid base-catalyzed autohydrolysis of the substrate. The fluorogenic substrate 4-methylumbelliferyl butyrate (4-MUB) showed less susceptibility to autohydrolysis at pH values of >9.0 and therefore was employed for the measurements.

The optimal temperatures for enzyme-catalyzed hydrolysis were determined to be around 47.7°C for EstB3 and 50°C for EstC7 (Fig. 5A). EstB3 showed a broader optimal pH range between 6.0 and 8.0, with a maximum at pH 7.0, whereas EstC7 had a narrow optimal pH range, with a maximum at pH 8.5 (Fig. 5B).

Downloaded from http://aem.asm.org/ on May 5, 2018 by guest

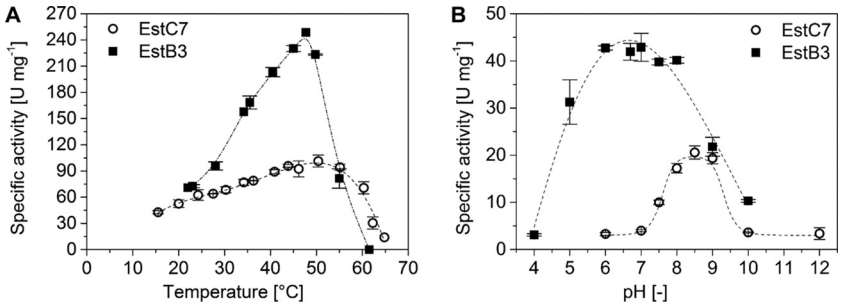


FIG 5 Temperature profiles (A) and pH profiles (B) of purified EstB3 and EstC7. Activities were measured as described in Materials and Methods, using *p*-nitrophenyl butyrate for the temperature measurements (at pH 7.5) and 4-methylumbelliferyl butyrate for pH measurements (at 30°C). Mean values of at least three separate measurements are shown; error bars indicate the standard deviations. For reactions at 34.2, 47.7, and 61.5°C with EstC7 in panel A, single measurements were performed.

Polyesterase activity of EstB3 and EstC7 with PBAT (milled and foil). The polyesterase activity was measured by employing purified esterases EstB3 and EstC7 (Fig. 6). Hydrolytic activities were normalized to the applied esterase concentration (0.6 μM).

The polyesterase activities of purified EstB3 and EstC7 with both milled PBAT (Fig. 6A) and PBAT foil (Fig. 6B) showed distinct hydrolysis patterns. After incubation with both enzymes and substrate forms, Ta and BTa were determined to be the main hydrolysis products. No BTaB was observed; however, accumulation of BTa was prominent for EstB3 with milled PBAT, with a 6-fold higher concentration of BTa (60.4 μM [101 mol mol of enzyme^{-1}]) versus Ta (8.0 μM [17 mol mol of enzyme^{-1}]). The total concentration of quantified products in the EstB3 reaction was higher with the milled substrate than with the substrate foil. In contrast, the total concentrations of quantified monomeric subunits for EstC7 were equal with the two substrate forms (318 μM [530 mol mole enzyme^{-1}]). Total concentrations of quantified products were higher in the reactions with purified esterases than in the reactions with cell-free lysates (Fig. 4), probably due to greater catalyst loads. An unexpected finding was the change in the product profiles for the reactions with purified EstB3 and EstC7, compared to the reactions with the respective cell-free lysates. The higher concentrations of hydrolysis products measured with purified enzymes led to greater accumulation of BTa (Fig. 6). A possible reason is inactivation of the esterase before BTa is hydrolyzed further to the monomeric subunits (Ta and B). In addition, although control and blank reaction values were subtracted in the cell-free lysate experiments, a synergistic effect between the esterases and other cell lysate components, leading to a different distribution of hydrolysis products and less accumulation of BTa with cell-free lysates, cannot be fully excluded. Purified EstC7 yielded higher concentrations of Ta overall, especially with the

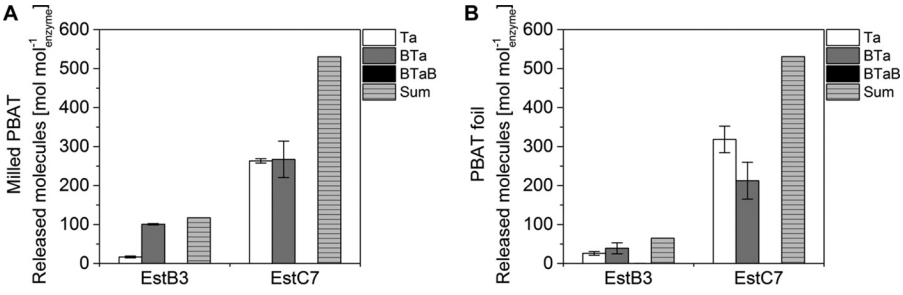


FIG 6 Hydrolysis of milled PBAT (A) and PBAT foil (B) by purified esterases EstB3 and EstC7. Reactions were performed as described in Materials and Methods (2-ml reaction mixtures at pH 7.5 with 0.6 μM enzyme, with incubation at 30°C and 150 rpm for 72 h). Hydrolysis products Ta, BTa, and BTaB were quantified by HPLC/UV-Vis analysis. The sum of products (Ta, BTa, and BTaB) is also given. Bars, mean values ($n = 3$); error bars, standard deviations.

Downloaded from http://aem.asm.org/ on May 5, 2018 by guest

PBAT foil (191.1 μM [318.5 mol mol of enzyme^{-1}]), indicating more efficient hydrolysis to the monomeric subunits and more effective hydrolysis of the aromatic Ta-B ester bond. Similar differences in hydrolytic cleavage patterns for aliphatic-aromatic polyesters between enzymes were reported previously, for example, for the cutinases from *Humicola insolens* (HiC) and *Thermobifida cellulosilytica* (Thc_Cut1). The cutinase Thc_Cut1 shows greater specificity for the hydrolysis of aromatic ester bonds (Ta-B) than does the cutinase HiC (12). Moreover, the polyesterase activities of the novel enzymes EstB3 and EstC7 with milled PBAT were significantly higher than the activities of the recently presented esterases from the anaerobic bacteria *Clostridium hathewayi* (Chath_Est1) (21) and *Clostridium botulinum* (Cbotu_Est and Cbotu_EstB) (20).

Conclusion. The plant-associated microbiome of moss plantlets was successfully investigated as a source of novel enzymes. To date, only a few examples reporting the identification of enzymes in plant-associated microbiomes through functional metagenomics are available (27). Moreover, we demonstrate here the hydrolytic activities of esterases obtained from a plant-associated microbiome with a synthetic copolyester. EstB3 and EstC7 showed significant hydrolytic activities with the synthetic aliphatic-aromatic copolyester PBAT. Since EstB3 and EstC7 belong to family VIII of carboxylesterases, polyesterase activity emerges as an unusual activity of this lipolytic enzyme family. In particular, EstC7 showed a strong preference for cleavage of the aromatic (Ta-B) ester bond, which is an attractive and challenging hydrolytic activity for degradation or modification of polyester-based materials.

MATERIALS AND METHODS

Chemicals and reagents. Milled PBAT, with a melting point of 125.3°C, a glass transition temperature of −34°C, a molecular number average of 19,000 g mol^{-1}, and a molecular weight average of 65,000 g mol^{-1}, milled to a particle size of 100 to 300 μm as described elsewhere (12), and PBAT foil (ecoflex, with a film thickness of 50 μm) were kindly provided by BASF SE. BaBTaBBa, with a particle size of 100 to 300 μm, BTaB, and BTa were synthesized and purified according to the methods described by Perz et al. (49). Amorphous solvent-casted polyethylene terephthalate films (film thickness of 0.25 mm) were purchased from Goodfellow (United Kingdom). The polymers used were of analytical grade, in order to exclude any influences of additives. All other chemicals were of analytical grade and purchased from Sigma-Aldrich (Germany), TCI Europe (Germany), Carl Roth (Germany), or Merck (Germany). DNA-modifying enzymes were obtained from New England BioLabs (Germany) or Thermo Scientific (Germany) and oligonucleotides from Sigma-Aldrich (Germany). Plasmid DNA was isolated using the GeneJet plasmid miniprep kit (Thermo Scientific). The Wizard SV PCR cleanup kit (Promega, USA) was used for purification and agarose gel extraction of PCR products.

Initial screening of the *Sphagnum* moss metagenome library. The microbiome of moss (*Sphagnum magellanicum*) from a sampling site in the Alpine bog Pirker Waldhochmoor (N46°37′38.66″, E14°26′5.66″) in Austria was employed for extraction of metagenomic DNA and generation of a fosmid clone library using the CopyControl fosmid library production kit (Epicentre), as described previously (50). Activity screening of the fosmid library in *E. coli* EPI300 pCC2FOS (Epicentre) was performed on LB medium (pH 7.5) agar plates containing 1% (vol/vol) tributyrin (emulsified using an Ultra Turrax homogenizer [IKA Werke, Germany]), 15 g liter^{-1} agar, 1.2 g liter^{-1} gum arabic, 1× fosmid autoinduction solution (Epicentre), and 12.5 μg ml^{-1} chloramphenicol. The plates were incubated at 30°C for up to 7 days until a clear zone (halo) was detected around the colonies. Positive clones were evaluated for esterase activity using cell-free lysates and the soluble esterase substrate *p*NPB.

Preparation of cell-free lysates. Fosmid clones (*E. coli* EPI300) were cultured at 30°C at 120 rpm for 16 h in 50 ml LB medium containing 1× fosmid autoinduction solution (Epicentre, USA) and 12.5 μg ml^{-1} chloramphenicol. Cells were harvested by centrifugation (2,900 × *g* at 4°C for 15 min). Cell pellets from 50- or 400-ml cultures were resuspended in 6 or 40 ml, respectively, of 0.1 M Tris-HCl buffer (pH 7.5). Cell-free lysates were prepared by sonication (twice for 1 min, at 45% amplitude) with a digital sonifier (Branson, USA), followed by lysis in a FastPrep instrument (MP Biomedicals, USA) for 60 s at 6.0 m s^{-1}, using 20% (vol/vol) glass beads (0.1 to 0.25 mm; Retsch GmbH, Germany). Cell debris was removed by centrifugation (16,000 × *g* at 4°C for 30 min), and lysates were filtered (0.45 μm; Roth, Germany) and stored at 4°C until further use. For polyester degradation assays, lysates were shock-frozen in liquid nitrogen and lyophilized for 48 h in a FreeZone 4.5 freeze dryer (Labconco, USA).

Subcloning, sequencing of fosmids, and cloning of esterases. A subclone library of each fosmid was prepared by restriction of isolated plasmids with EcoRI and HindIII for B11, C5, C7, C9, and G4 or BamHI for B3, followed by cleanup of restriction products, ligation into the same vector backbone used for library construction (pCC2FOS), and transformation into the library strain *E. coli* EPI300 (Epicentre). Clones were subjected again to activity screening on tributyrin agar plates, as described above. From each subclone library, one colony displaying halo formation was selected for sequencing by primer walking at LGC Genomics (Germany) or Microsynth (Switzerland). Primers used for the initial sequencing are specified in Table S1 in the supplemental material. CLC Main Workbench software (Qiagen) was

Downloaded from http://aem.asm.org/ on May 5, 2018 by guest

employed for sequence assembly, BLASTX analysis, and identification of ORFs. The esterase-coding genes for EstB11, EstC5, EstC7, EstC9, and EstG4 were cloned into pET28a(+) (Novagen, USA) through restriction cloning, while EstB3 was cloned with a ligase-independent method (phosphorothioate-based ligase-independent gene cloning [PLICing]), as described elsewhere (51). A standard PCR mixture (50 μl) contained 1× Phusion HF buffer, 1 U of Phusion DNA polymerase (New England BioLabs), 0.2 mM deoxynucleoside triphosphates, 0.2 μM each primer, and 10 ng of plasmid DNA. The PCR primers employed are listed in Table S1. Ligated/hybridized plasmids were transformed into chemically competent *E. coli* BL21(DE3) cells (Invitrogen, USA) and *E. coli* Lemo21(DE3) cells (New England BioLabs, Germany).

Protein expression. The strains employed for expression of the six cloned esterases in pET28a(+) were *E. coli* Lemo21(DE3) for EstB3, EstB11, EstC5, EstC9, and EstG4 and *E. coli* BL21(DE3) for EstC7. For control reactions, *E. coli* strains BL21(DE3) and Lemo(DE3) containing the empty vector pET28a(+) were cultivated under the same conditions. Flasks containing 400 ml of LB medium, 50 μg ml^{-1} kanamycin, and 12.5 μg ml^{-1} chloramphenicol [for Lemo21(DE3) strains] were inoculated with 2% (vol/vol) of an overnight culture and incubated at 37°C and 120 rpm until the respective optical density at 600 nm (OD_{600}) was obtained (OD_{600} of 0.6 for EstB3 and OD_{600} of 0.8 for the remaining strains). Protein expression was induced by the addition of isopropyl-β-D-thiogalactopyranoside (IPTG) (1 mM for EstB11 and EstC5 and 0.4 mM for the remaining strains). Cultures containing EstB3, EstB11, EstC5, and EstC7 were incubated further at 25°C and 200 rpm, and those containing EstC9, EstG4, and the empty vector controls were incubated at 30°C and 200 rpm. The optimal incubation time after induction was 4 h for EstC7, EstC9, and EstG4, 5 h for EstB3, and 20 h for EstB11 and EstC5. Additionally, in the case of EstB3, 0.5 mM L-rhamnose was added upon induction and agitation was performed at 240 rpm. Cell-free lysates for activity assays were prepared as indicated above.

Esterase activity assay with *p*-nitrophenyl butyrate. Hydrolytic activity was assayed spectrophotometrically at 410 nm and 30°C using a U-2001 spectrophotometer (Hitachi, Japan) or a Tecan M200 plate reader (Tecan, Switzerland). A typical reaction mixture contained 0.5 mM *p*NPB, 5% (vol/vol) acetonitrile as cosolvent, and 50 μl of cell-free lysate (65 to 250 μg total protein) or 0.2 to 2.5 μg purified enzyme, in a final volume of 1 ml (cuvette) or 200 μl (96-well plate) of 0.1 M Tris-HCl buffer (pH 7.5). The reaction was initiated by the addition of enzyme or lysate. One unit was defined as the amount of activity required for the release of 1 μmol of *p*-nitrophenol per minute. The initial hydrolysis rates (linear signal, up to 20 s) were employed for activity determination. Concentrations of 3.12 to 100 μM *p*-nitrophenol (extinction coefficient of 10.2 mM^{-1} cm^{-1}) were used to generate a calibration curve.

Detection of active serine hydrolases by SDS-PAGE and fluorescence labeling. In order to identify serine hydrolases in cell-free lysates and purified proteins, SDS-PAGE was performed according to the method described by Laemmli (52). Protein samples were pretreated with the ActiveX 6-carboxytetramethylrhodamine fluorophosphonate (TAMRA-FP) serine hydrolase probe (Thermo Scientific, USA), according to the manufacturer's protocol, to label active serine hydrolases prior to SDS-PAGE separation. After fluorescence imaging of the gel with a Cy3 filter to detect labeled serine hydrolases, proteins were stained with Coomassie brilliant blue R-250. The PageRuler prestained protein ladder (10 to 170 kDa; Thermo Scientific, Germany) was used as a molecular mass marker.

Screening for polyester hydrolytic activity using PBAT, model substrate BaBTaBBa, and PET. Cell-free lysates of nonredundant fosmid clones (clones B3, B11, C5, C7, C9, and G4) were evaluated for their hydrolytic activities with milled PBAT and the oligomeric model substrate BaBTaBBa. Lyophilized cell-free lysates (80 to 84 mg, from 50-ml cultures) were redissolved in 3.5 ml double-distilled water (ddH_2O) to obtain a 0.17 M Tris-HCl buffered solution (pH 7.5). Esterase activity of the samples was first confirmed with the *p*NPB assay. Rehydrated lysates (1 ml; 23 to 24 g liter^{-1}) were incubated for 72 h at 30°C and 100 rpm with 10 mg milled PBAT, 7 mg BaBTaBBa, or PET foil (0.5 by 1 cm), followed by RP-HPLC/UV-Vis analysis. Prior to incubation, PET foils were washed as described previously (45).

Substrate specificity for *p*-nitrophenyl aliphatic esters. Esterase activity toward *p*-nitrophenyl aliphatic esters with different chain lengths was determined according to the standard ester-hydrolyzing activity assay described for *p*NPB, using a U-2001 spectrophotometer (Hitachi). Hydrolytic activity was measured using the following *p*NP esters: *p*NP acetate ($pNPC_2$), *p*NPB ($pNPC_4$), *p*NP hexanoate ($pNPC_6$), *p*NP octanoate ($pNPC_8$), *p*NP decanoate ($pNPC_{10}$), *p*NP dodecanoate ($pNPC_{12}$), and *p*NP palmitate ($pNPC_{16}$). To enable comparison of the substrate profiles using cell-free lysates, independent of different expression levels in each lysate, volumetric activities (units per liter) were calculated as percentages of the activity with the reference substrate *p*NPB. For purified enzymes (EstB3 and EstC7), the hydrolytic activity was calculated as units per milligram of enzyme. To increase the solubility of the long-chain and less-soluble substrates and to provide equal conditions for all reactions, 1% (vol/vol) Triton X-100 was added to the reaction buffer. The reactions in 0.1 M Tris-HCl buffer (pH 7.5) contained 0.5 mM *p*NP substrate, 5% (vol/vol) acetonitrile, 1% (vol/vol) Triton X-100, and cell-free lysate or purified enzyme. For purified enzymes, protein concentrations were measured using the Pierce bicinchoninic acid (BCA) protein assay kit (Thermo Scientific), with bovine serum albumin as the protein standard. Background activity was measured in a blank reaction without the addition of lysate. Moreover, control reactions were performed using lysates of *E. coli* carrying the empty vector. The sample signals were then corrected by subtraction of the background and control reaction signals.

Thermostability (residual activity). The thermostability of the six cloned and expressed esterases was measured using sterile filtered cell-free lysates. The lysates were incubated continuously at 30°C and 50°C for 168 h and 96 h, respectively. Samples were withdrawn upon initiation of the incubation (initial activity), after 6 h, and every 24 h. Initial and residual activities were measured in triplicate using the *p*NPB

Downloaded from http://aem.asm.org/ on May 5, 2018 by guest

assay, as described above. Control reactions using cell-free lysates of *E. coli* carrying the empty vector were performed simultaneously, and results were subtracted from the sample signals.

Purification of EstC7 and EstB3. His-tagged esterases EstC7 and EstB3 were purified under nondenaturing conditions using a 1-ml HisTrap HP column (GE Health Care, USA), according to the manufacturer's protocol. After expression, cell pellets were resuspended in 14 ml of 20 mM Tris-HCl buffer (pH 7.0) containing 0.5 M NaCl and 50 mM imidazole. Cell-free lysates were prepared as described above. Fractions containing active esterase were eluted with 500 and 750 mM imidazole for EstC7 and EstB3, respectively. Buffer exchange was performed through dilution and centrifugation using Amicon Ultra-15 centrifugal filters (10-kDa cutoff; Merck Millipore), using 20 mM Tris-HCl buffer (pH 7.0) containing 0.5 M NaCl. For the polyesterase activity determination, the purified enzymes were shock-frozen in liquid nitrogen and lyophilized as described above.

Temperature optima, pH optima, and kinetic characterization of EstC7 and EstB3. Kinetic data (K_m and V_{max}) were recorded at 30°C and pH 7.5, using purified enzyme (0.78 to 1,000 μM) and the *p*NPB assay described above. Protein concentrations were measured using the Pierce BCA protein assay kit (Thermo Scientific), with bovine serum albumin as the protein standard. Specific activities are given as units per milligram of enzyme. Temperature optima were also determined using the *p*NPB assay, at a pH of 7.5 and various temperatures (15 to 64°C). For the pH-dependent activity measurements, the more suitable fluorogenic substrate 4-MUB was employed, since the chromogenic substrate *p*NPB is more susceptible to autohydrolysis above pH 9, making measurements at pH values of >9 unfeasible. The 4-MUB assay consisted of 0.5 mM 4-MUB in 0.2 ml of the Britton-Robinson universal buffer system (40 mM acetic acid, 40 mM phosphoric acid, and 40 mM boracic acid, at pH values of 5.0 to 12.0). The reaction was started by the addition of enzyme. The increase in fluorescence was recorded using a Tecan M200 plate reader, and quantification was performed using a 4-methylumbelliferone standard curve for each pH value. The signal was corrected for autohydrolysis of the substrate at each pH by subtracting the background signal (control reaction without enzyme). One unit was defined as the amount of activity required for the release of 1 μmol of 4-methylumbelliferone per minute.

Polyesterase activity of all six esterases (cell-free lysates) and purified EstB3 and EstC7 with PBAT (milled and foil). Lyophilized cell-free lysates (0.3 g, from 200-ml cultures) from *E. coli* Lemo21(DE3) or *E. coli* BL21(DE3) containing the expressed esterases or the empty vector (control reaction) and Tris-HCl buffer were resuspended in 13 ml ddH_2O, while lyophilized purified enzymes EstB3 (48.08 kDa) and EstC7 (43.74 kDa) were dissolved in ddH_2O to yield an enzyme concentration of 0.6 μM. The reaction mixtures had a final pH of 7.5 and contained one piece of PBAT foil (0.5 by 1 cm) or 10 mg milled PBAT in 2 ml of rehydrated cell-free lysate (23.1 g liter^{-1}) or 2 ml of purified enzyme (0.6 μM). Samples were incubated at 30°C and 150 rpm for 72 h, followed by HPLC analysis. Blank reactions, without the addition of resuspended cell-free lysates or purified enzymes, and control reactions, containing resuspended cell-free lysates of *E. coli* carrying the empty vector, were performed simultaneously. The concentrations of hydrolysis products released during control and blank reactions were subtracted from the concentrations reached in sample reactions in order to exclude the influence of hydrolytic enzymes from the *E. coli* host.

HPLC quantification of released hydrolysis products. Hydrolysis reactions were stopped by methanol precipitation through the addition of 0.5 ml of ice-cooled methanol to 0.5-ml sample, control, and blank reaction mixtures. The hydrolysis products Ta, Ada, benzoic acid (Ba), BTa, and BTaB were quantified by means of RP-HPLC using a Dionex system (Dionex, USA), consisting of an UltiMate 3000 pump, an ASI-100 automated sample injector, an UltiMate 3000 column compartment, and a UVD 340U photodiode array detector, in combination with a XTerra RP_{18} column (3.5 μm; 3.0 mm by 150 mm) with a precolumn (Waters Corp., USA). Separation of the hydrolysis products was performed as described previously (12). Signals from blank and control reactions were subtracted from the sample signals in order to correct the data for background activity (autohydrolysis). Quantification of hydrolysis products was performed using calibration curves constructed with authentic standards.

Phylogenetic analysis. Phylogenetic analysis on the basis of amino acid sequence similarities was performed using sequences from closest hits from BLASTX analysis with the NCBI GenBank protein database. Multiple sequence alignments were performed using ClustalW software (53), Gonnet protein weight matrices, and default parameters, with visualization by ESPript 3.0 (54). A neighbor-joining phylogenetic tree was constructed with MEGA6 software (55), using the number-of-differences method and a bootstrap of 1,000 replicates. Positions containing gaps and missing data were eliminated, which yielded a total of 92 positions in the final data set.

Accession number(s). The nucleotide sequences were deposited in the GenBank database under the following accession numbers: KX533504 for EstB3, KX533505 for EstB11, KX533506 for EstC5, KX533507 for EstC7, KX533508 for EstC9, and KX533509 for EstG4.

SUPPLEMENTAL MATERIAL

Supplemental material for this article may be found at https://doi.org/10.1128/AEM.02641-16.

TEXT S1, PDF file, 3.1 MB.

ACKNOWLEDGMENTS

This work was supported by the Federal Ministry of Science, Research, and Economy, the Federal Ministry of Traffic, Innovation, and Technology, the Styrian Business Pro-

Downloaded from http://aem.asm.org/ on May 5, 2018 by guest

motion Agency, the Standortagentur Tirol, the Government of Lower Austria, and the Technology Agency of the City of Vienna through the COMET Funding Program, managed by the Austrian Research Promotion Agency.

We thank Cornelia Rainer, Tanja Nottendorfer, and Christina Laireiter (Graz University of Technology), as well as Johanna Aigner (FH Joanneum Graz), for valuable support and Daria Rybakova (Graz University of Technology) for proofreading of the manuscript and valuable discussions.

REFERENCES

1. Lee SY. 1996. Bacterial polyhydroxyalkanoates. Biotechnol Bioeng 49:1–14. https://doi.org/10.1002/(SICI)1097-0290(19960105)49:1<1::AID-BIT1>3.3.CO;2-1.
2. Pollard M, Beisson F, Li Y, Ohlrogge JB. 2008. Building lipid barriers: biosynthesis of cutin and suberin. Trends Plant Sci 13:236–246. https://doi.org/10.1016/j.tplants.2008.03.003.
3. Witt U, Müller R-J, Deckwer W-D. 1995. New biodegradable polyester-copolymers from commodity chemicals with favorable use properties. J Environ Polym Degrad 3:215–223. https://doi.org/10.1007/BF02068676.
4. Mueller R-J. 2006. Biological degradation of synthetic polyesters: enzymes as potential catalysts for polyester recycling. Process Biochem 41:2124–2128. https://doi.org/10.1016/j.procbio.2006.05.018.
5. Woodall LC, Sanchez-Vidal A, Canals M, Paterson GLJ, Coppock R, Sleight V, Calafat A, Rogers AD, Narayanaswamy BE, Thompson RC. 2014. The deep sea is a major sink for microplastic debris. R Soc Open Sci 1:140317. https://doi.org/10.1098/rsos.140317.
6. Zimmermann W, Billig S. 2010. Enzymes for the biofunctionalization of poly(ethylene terephthalate), p 97–120. *In* Nyanhongo GS, Steiner W, Gübitz G (ed), Biofunctionalization of polymers and their applications. Springer, Berlin, Germany.
7. Marten E, Müller R-J, Deckwer W-D. 2003. Studies on the enzymatic hydrolysis of polyesters. I. Low molecular mass model esters and aliphatic polyesters. Polym Degrad Stab 80:485–501.
8. Marten E, Müller R-J, Deckwer W-D. 2005. Studies on the enzymatic hydrolysis of polyesters. II. Aliphatic-aromatic copolyesters. Polym Degrad Stab 88:371–381.
9. Vroman I, Tighzert L. 2009. Biodegradable polymers. Materials 2:307–344. https://doi.org/10.3390/ma2020307.
10. Weng Y-X, Jin Y-J, Meng Q-Y, Wang L, Zhang M, Wang Y-Z. 2013. Biodegradation behavior of poly(butylene adipate-co-terephthalate) (PBAT), poly(lactic acid) (PLA), and their blend under soil conditions. Polym Test 32:918–926. https://doi.org/10.1016/j.polymertesting.2013.05.001.
11. Kleeberg I, Hetz C, Kroppenstedt RM, Müller R-J, Deckwer W-D. 1998. Biodegradation of aliphatic-aromatic copolyesters by *Thermonospora fusca* and other thermophilic compost isolates. Appl Environ Microbiol 64:1731–1735.
12. Perz V, Bleymaier K, Sinkel C, Kueper U, Bonnekessel M, Ribitsch D, Guebitz GM. 2016. Substrate specificities of cutinases on aliphatic-aromatic polyesters and on their model substrates. New Biotechnol 33:295–304. https://doi.org/10.1016/j.nbt.2015.11.004.
13. Wohlgemuth R. 2010. Large-scale applications of hydrolases in biocatalytic asymmetric synthesis, p 249–264. *In* Blaser HU, Federsel H-J (ed), Asymmetric catalysis on industrial scale: challenges, approaches and solutions, 2nd ed. Wiley-VCH, Weinheim, Germany.
14. Arpigny JL, Jaeger K-E. 1999. Bacterial lipolytic enzymes: classification and properties. Biochem J 343:177–183. https://doi.org/10.1042/bj3430177.
15. Rao L, Xue Y, Zhou C, Tao J, Li G, Lu JR, Ma Y. 2011. A thermostable esterase from *Thermoanaerobacter tengcongensis* opening up a new family of bacterial lipolytic enzymes. Biochim Biophys Acta 1814:1695–1702. https://doi.org/10.1016/j.bbapap.2011.08.013.
16. Tokiwa Y, Suzuki T. 1977. Hydrolysis of polyesters by lipases. Nature 270:76–78. https://doi.org/10.1038/270076a0.
17. Ronkvist ÅM, Xie W, Lu W, Gross RA. 2009. Cutinase-catalyzed hydrolysis of poly(ethylene terephthalate). Macromolecules 42:5128–5138. https://doi.org/10.1021/ma9005318.
18. Ribitsch D, Heumann S, Trotscha E, Herrero Acero E, Greimel K, Leber R, Birner-Gruenberger R, Deller S, Eiteljoerg I, Remler P, Weber T, Siegert P, Maurer K-H, Donelli I, Freddi G, Schwab H, Guebitz GM. 2011. Hydrolysis of polyethyleneterephthalate by *p*-nitrobenzylesterase from *Bacillus subtilis*. Biotechnol Prog 27:951–960. https://doi.org/10.1002/btpr.610.
19. Kawai F, Oda M, Tamashiro T, Waku T, Tanaka N, Yamamoto M, Mizushima H, Miyakawa T, Tanokura M. 2014. A novel Ca^{2+}-activated, thermostabilized polyesterase capable of hydrolyzing polyethylene terephthalate from *Saccharomonospora viridis* AHK190. Appl Microbiol Biotechnol 98:10053–10064. https://doi.org/10.1007/s00253-014-5860-y.
20. Perz V, Baumschlager A, Bleymaier K, Zitzenbacher S, Hromic A, Steinkellner G, Pairitsch A, Łyskowski A, Gruber K, Sinkel C, Küper U, Ribitsch D, Guebitz GM. 2016. Hydrolysis of synthetic polyesters by *Clostridium botulinum* esterases. Biotechnol Bioeng 113:1024–1034. https://doi.org/10.1002/bit.25874.
21. Perz V, Hromic A, Baumschlager A, Steinkellner G, Pavkov-Keller T, Gruber K, Bleymaier K, Zitzenbacher S, Zankel A, Mayrhofer C, Sinkel C, Kueper U, Schlegel K, Ribitsch D, Guebitz GM. 2016. An esterase from anaerobic *Clostridium hathewayi* can hydrolyze aliphatic-aromatic polyesters. Environ Sci Technol 50:2899–2907. https://doi.org/10.1021/acs.est.5b04346.
22. Yoshida S, Hiraga K, Takehana T, Taniguchi I, Yamaji H, Maeda Y, Toyohara K, Miyamoto K, Kimura Y, Oda K. 2016. A bacterium that degrades and assimilates poly(ethylene terephthalate). Science 351:1196–1199. https://doi.org/10.1126/science.aad6359.
23. Ferrer M, Golyshina OV, Chernikova TN, Khachane AN, Martins dos Santos VAP, Yakimov MM, Timmis KN, Golyshin PN. 2005. Microbial enzymes mined from the Urania deep-sea hypersaline anoxic basin. Chem Biol 12:895–904. https://doi.org/10.1016/j.chembiol.2005.05.020.
24. Sulaiman S, Yamato S, Kanaya E, Kim J-J, Koga Y, Takano K, Kanaya S. 2012. Isolation of a novel cutinase homolog with polyethylene terephthalate-degrading activity from leaf-branch compost by using a metagenomic approach. Appl Environ Microbiol 78:1556–1562. https://doi.org/10.1128/AEM.06725-11.
25. Mayumi D, Akutsu-Shigeno Y, Uchiyama H, Nomura N, Nakajima-Kambe T. 2008. Identification and characterization of novel poly(DL-lactic acid) depolymerases from metagenome. Appl Microbiol Biotechnol 79:743–750. https://doi.org/10.1007/s00253-008-1477-3.
26. Tchigvintsev A, Tran H, Popovic A, Kovacic F, Brown G, Flick R, Hajighasemi M, Egorova O, Somody JC, Tchigvintsev D, Khusnutdinova A, Chernikova TN, Golyshina OV, Yakimov MM, Savchenko A, Golyshin PN, Jaeger K-E, Yakunin AF. 2015. The environment shapes microbial enzymes: five cold-active and salt-resistant carboxylesterases from marine metagenomes. Appl Microbiol Biotechnol 99:2165–2178. https://doi.org/10.1007/s00253-014-6038-3.
27. Müller CA, Obermeier MM, Berg G. 2016. Bioprospecting plant-associated microbiomes. J Biotechnol 235:171–180. https://doi.org/10.1016/j.jbiotec.2016.03.033.
28. Berg G, Grube M, Schloter M, Smalla K. 2014. Unraveling the plant microbiome: looking back and future perspectives. Front Microbiol 5:148. https://doi.org/10.3389/fmicb.2014.00148.
29. Raghoebarsing AA, Smolders AJP, Schmid MC, Rijpstra WIC, Wolters-Arts M, Derksen J, Jetten MSM, Schouten S, Sinninghe Damsté JS, Lamers LPM, Roelofs JGM, Op den Camp HJM, Strous M. 2005. Methanotrophic symbionts provide carbon for photosynthesis in peat bogs. Nature 436:1153–1156. https://doi.org/10.1038/nature03802.
30. Opelt K, Chobot V, Hadacek F, Schönmann S, Eberl L, Berg G. 2007. Investigations of the structure and function of bacterial communities associated with *Sphagnum* mosses. Environ Microbiol 9:2795–2809. https://doi.org/10.1111/j.1462-2920.2007.01391.x.
31. Bragina A, Oberauner-Wappis L, Zachow C, Halwachs B, Thallinger GG, Müller H, Berg G. 2014. The *Sphagnum* microbiome supports bog ecosystem functioning under extreme conditions. Mol Ecol 23:4498–4510. https://doi.org/10.1111/mec.12885.
32. Moore T, Basiliko N. 2006. Decomposition in boreal peatlands, p

Downloaded from http://aem.asm.org/ on May 5, 2018 by guest

125–143. *In* Wieder RK, Vitt DH (ed), Boreal peatland ecosystems. Springer, Berlin, Germany.
33. Hájek T, Ballance S, Limpens J, Zijlstra M, Verhoeven JTA. 2010. Cell-wall polysaccharides play an important role in decay resistance of *Sphagnum* and actively depressed decomposition in vitro. Biogeochemistry 103: 45–57.
34. Steger D, Wentrup C, Braunegger C, Deevong P, Hofer M, Richter A, Baranyi C, Pester M, Wagner M, Loy A. 2011. Microorganisms with novel dissimilatory (bi)sulfite reductase genes are widespread and part of the core microbiota in low-sulfate peatlands. Appl Environ Microbiol 77:1231–1242. https://doi.org/10.1128/AEM.01352-10.
35. Kremer C, Pettolino F, Bacic A, Drinnan A. 2004. Distribution of cell wall components in *Sphagnum* hyaline cells and in liverwort and hornwort elaters. Planta 219:1023–1035. https://doi.org/10.1007/s00425-004-1308-4.
36. Popper ZA. 2008. Evolution and diversity of green plant cell walls. Curr Opin Plant Biol 11:286–292. https://doi.org/10.1016/j.pbi.2008.02.012.
37. Klavina L, Springe G, Nikolajeva V, Martsinkevich I, Nakurte I, Dzabijeva D, Steinberga I. 2015. Chemical composition analysis, antimicrobial activity and cytotoxicity screening of moss extracts (moss phytochemistry). Molecules 20:17221–17243. https://doi.org/10.3390/molecules200917221.
38. Petersen TN, Brunak S, von Heijne G, Nielsen H. 2011. SignalP 4.0: discriminating signal peptides from transmembrane regions. Nat Methods 8:785–786. https://doi.org/10.1038/nmeth.1701.
39. Cha S-S, An YJ, Jeong C-S, Kim M-K, Jeon JH, Lee C-M, Lee HS, Kang SG, Lee J-H. 2013. Structural basis for the β-lactamase activity of EstU1, a family VIII carboxylesterase. Proteins 81:2045–2051. https://doi.org/10.1002/prot.24334.
40. Jeon JH, Kim S-J, Lee HS, Cha S-S, Lee JH, Yoon S-H, Koo B-S, Lee C-M, Choi SH, Lee SH, Kang SG, Lee J-H. 2011. Novel metagenome-derived carboxylesterase that hydrolyzes β-lactam antibiotics. Appl Environ Microbiol 77:7830–7836. https://doi.org/10.1128/AEM.05363-11.
41. Mokoena N, Mathiba K, Tsekoa T, Steenkamp P, Rashamuse K. 2013. Functional characterisation of a metagenome derived family VIII esterase with a deacetylation activity on β-lactam antibiotics. Biochem Biophys Res Commun 437:342–348.
42. Upton C, Buckley JT. 1995. A new family of lipolytic enzymes? Trends Biochem Sci 20:178–179. https://doi.org/10.1016/S0968-0004(00)89002-7.
43. Hemilä H, Koivula TT, Palva I. 1994. Hormone-sensitive lipase is closely related to several bacterial proteins, and distantly related to acetylcholinesterase and lipoprotein lipase: identification of a superfamily of esterases and lipases. Biochim Biophys Acta 1210:249–253. https://doi.org/10.1016/0005-2760(94)90129-5.
44. Biundo A, Hromic A, Pavkov-Keller T, Gruber K, Quartinello F, Haernvall K, Perz V, Arrell MS, Zinn M, Ribitsch D, Guebitz GM. 2016. Characterization of a poly(butylene adipate-co-terephthalate)-hydrolyzing lipase from *Pelosinus fermentans*. Appl Microbiol Biotechnol 100:1753–1764. https://doi.org/10.1007/s00253-015-7031-1.
45. Herrero Acero E, Ribitsch D, Steinkellner G, Gruber K, Greimel K, Eiteljoerg I, Trotscha E, Wei R, Zimmermann W, Zinn M, Cavaco-Paulo A, Freddi G, Schwab H, Guebitz G. 2011. Enzymatic surface hydrolysis of PET: effect of structural diversity on kinetic properties of cutinases from *Thermobifida*. Macromolecules 44:4632–4640. https://doi.org/10.1021/ma200949p.
46. Ferrer M, Bargiela R, Martínez-Martínez M, Mir J, Koch R, Golyshina OV, Golyshin PN. 2015. Biodiversity for biocatalysis: a review of the α/β-hydrolase fold superfamily of esterases-lipases discovered in metagenomes. Biocatal Biotransformation 33:235–249. https://doi.org/10.3109/10242422.2016.1151416.
47. Rashamuse K, Magomani V, Ronneburg T, Brady D. 2009. A novel family VIII carboxylesterase derived from a leachate metagenome library exhibits promiscuous β-lactamase activity on nitrocefin. Appl Microbiol Biotechnol 83:491–500. https://doi.org/10.1007/s00253-009-1895-x.
48. Stoops JK, Hamilton SE, Zerner B. 1975. Carboxylesterases (EC 3.1.1): a comparison of some kinetic properties of horse, sheep, chicken, pig, and ox liver carboxylesterases. Can J Biochem 53:565–573. https://doi.org/10.1139/o75-077.
49. Perz V, Bleymaier K, Sinkel C, Kueper U, Bonnekessel M, Ribitsch D, Guebitz GM. 2016. Data on synthesis of oligomeric and polymeric poly(butylene adipate-co-butylene terephthalate) model substrates for the investigation of enzymatic hydrolysis. Data Brief 7:291–298. https://doi.org/10.1016/j.dib.2016.02.029.
50. Müller CA, Oberauner-Wappis L, Peyman A, Amos GCA, Wellington EMH, Berg G. 2015. Mining for nonribosomal peptide synthetase and polyketide synthase genes revealed a high level of diversity in the *Sphagnum* bog metagenome. Appl Environ Microbiol 81:5064–5072. https://doi.org/10.1128/AEM.00631-15.
51. Blanusa M, Schenk A, Sadeghi H, Marienhagen J, Schwaneberg U. 2010. Phosphorothioate-based ligase-independent gene cloning (PLICing): an enzyme-free and sequence-independent cloning method. Anal Biochem 406:141–146. https://doi.org/10.1016/j.ab.2010.07.011.
52. Laemmli UK. 1970. Cleavage of structural proteins during the assembly of the head of bacteriophage T4. Nature 227:680–685. https://doi.org/10.1038/227680a0.
53. Thompson JD, Higgins DG, Gibson TJ. 1994. CLUSTAL W: improving the sensitivity of progressive multiple sequence alignment through sequence weighting, position-specific gap penalties and weight matrix choice. Nucleic Acids Res 22:4673–4680. https://doi.org/10.1093/nar/22.22.4673.
54. Robert X, Gouet P. 2014. Deciphering key features in protein structures with the new ENDscript server. Nucleic Acids Res 42:W320–W324. https://doi.org/10.1093/nar/gku316.
55. Tamura K, Stecher G, Peterson D, Filipski A, Kumar S. 2013. MEGA6: Molecular Evolutionary Genetics Analysis version 6.0. Mol Biol Evol 30:2725–2729. https://doi.org/10.1093/molbev/mst197.

Downloaded from http://aem.asm.org/ on May 5, 2018 by guest